

Time-Dependent Density Functional Molecular Orbital and Excited State Calculations on Bis(porphyrinyl)butadiynes in the Monocationic, Neutral, Monoanionic, and Dianionic Oxidation States

Gregory J. Wilson and Dennis P. Arnold*

School of Physical and Chemical Sciences, Queensland University of Technology, G.P.O. Box 2434, Brisbane, Australia 4001

Received: February 8, 2005; In Final Form: May 12, 2005

We report a theoretical study of the multiple oxidation states (1+, 0, 1−, and 2−) of a *meso,meso*-linked diporphyrin, namely bis[10,15,20-triphenylporphyrinatozinc(II)-5-yl]butadiyne (**4**), using Time-Dependent Density Functional Theory (TDDFT). The origin of electronic transitions of singlet excited states is discussed in comparison to experimental spectra for the corresponding oxidation states of the close analogue bis{10,15,20-tris[3',5'-di-*tert*-butylphenyl]porphyrinatozinc(II)-5-yl}butadiyne (**3**). The latter were measured in previous work under in situ spectroelectrochemical conditions. Excitation energies and orbital compositions of the excited states were obtained for these large delocalized aromatic radicals, which are unique examples of organic mixed-valence systems. The radical cations and anions of butadiyne-bridged diporphyrins such as **3** display characteristic electronic absorption bands in the near-IR region, which have been successfully predicted with use of these computational methods. The radicals are clearly of the “fully delocalized” or Class III type. The key spectral features of the neutral and dianionic states were also reproduced, although due to the large size of these molecules, quantitative agreement of energies with observations is not as good in the blue end of the visible region. The TDDFT calculations are largely in accord with a previous empirical model for the spectra, which was based simplistically on one-electron transitions among the eight key frontier orbitals of the C₄ (1,4-butadiyne) linked diporphyrins.

Introduction

Inspired by the elegant oligo(porphyrinoid) structures of the photosynthetic apparatus, chemists have pursued the construction and characterization of many oligo(porphyrin) structures. In general, those arrays in which the porphyrins are linked covalently by carbon bridges may be classified broadly into two types, namely (i) those in which there is little or no ground-state electronic interaction between the porphyrin π electron systems¹ and (ii) those in which strong delocalization is a feature of the structures.^{2–6} The former are better models of the natural photosynthetic pigment arrays because they exhibit interporphyrin communication that is weak in the ground state, yet strong in the excited states. However, the second class of molecules also has attractions for the fields of molecular electronics, light harvesting, nanosensing, and nonlinear optics, especially if the degree of delocalization can be controlled by judicious choice of the conjugated linker(s). For many years, we have been interested in porphyrins linked by conjugated alkynes, beginning with the bis(oep)butadiyne dinickel complex **1** (H₂oep = 2,3,7,8,12,13,17,18-octaethylporphyrin; M = M' = Ni).³ Several groups have since investigated this general class of compounds in detail, and a broad array of experimental techniques has been employed for their investigation.^{4–6} The major interest in these molecules lies in the potential ability of the alkyne or extended alkyne bridge to function as a conducting wire, which facilitates strong communication between the porphyrins, particularly when attached in the *meso* position(s).⁷ These molecules, especially when combined into oligomers,

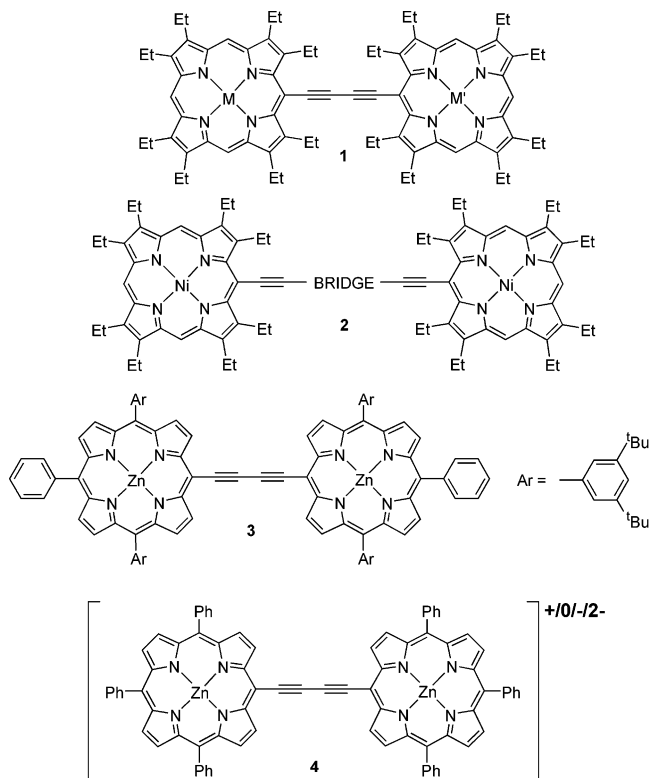
are very attractive for exploiting nonlinear optical phenomena such as two-photon absorption.⁸

The calculation of electronic structures of alkyne-linked diporphyrins has been performed previously with several approaches. Beljonne et al. used INDO/SCI and INDO/MRD-CI methods to simulate the optical responses of butadiyne-terminated, butadiyne-linked diporphyrins.⁹ Therien's group used ZINDO-CI to simulate the frontier molecular orbitals and energies in a suite of *meso-meso* ethyne-linked diporphyrins and recently applied semiempirical electronic structure calculations to a series of dinuclear porphyrins bridged by proquinoidal/alkynyl linkers.¹⁰ Zhou et al. computed the frontier orbitals of a series of dinuclear systems that they have used as the basis of two-photon absorbers.¹¹ Our own contribution to this field in 1996 was to use Density Functional Theory (DFT) to investigate the progression from the unsubstituted monoporphyrin through the *meso*-ethyne-substituted monoporphyrin to the butadiyne-linked diporphyrin, and to study the effects of the interporphyrin dihedral angle on the frontier orbital interactions.¹² In that work, due to constraints of computing power, we used the ligand stripped of substituents, i.e., the parent porphyrin.

In our previous synthetic, spectroscopic, and electrochemical studies, we proposed a semiquantitative empirical description of the frontier orbital manifold of the C₄ (1,4-butadiyne) linked diporphyrins.¹³ This was the result of our discovery of remarkably intense near-IR electronic absorption bands in the species derived by electrochemical reduction to the monoanion and dianion.¹⁴ This work was initially pursued with two series of bis(oep) complexes, the butadiynes **1** with various central metal ions and other dinickel complexes **2** with longer conjugated

* Corresponding author. E-mail: d.arnold@qut.edu.au. Fax: +61 7 3864 1804.

bridges.^{13–15} More recently, we overcame an aggregation problem with our previous compounds by employing a tri-arylporphyrin ligand, and for the dizinc(II) system **3** [Ar = 3',5'-di(*tert*-butyl)phenyl], we were able to observe the electronic spectra of the molecule in four oxidation states, namely 1+, 0, 1-, and 2-, and showed the strong homology between the spectra of the two odd-electron states.¹⁶



Our objectives in the present theoretical study are to extend molecular orbital calculations on these systems to cover the molecule in all four oxidation states, and to test various significant points. Do the calculations predict the existence of near-IR bands, and how closely do the energies and intensities match the experimental results? What is the composition of the excited states that lead to the major absorption bands, particularly those in the visible to near-IR region, and how closely do the calculations match our earlier approximate description? These dumb-bell shaped molecules comprise two chromophores linked by a bridge, so another notable point is that the monoanion and -cation could be regarded as unique examples of “organic mixed-valence systems”. Such species have not been investigated as extensively as their metal-centered analogues,¹⁷ yet they may have future applications in molecular computing arrays. The degree of delocalization and the description of the interporphyrin interaction in “mixed-valence” parlance are therefore important. This is pertinent for these diporphyrins, because while they appear to possess very strong delocalization through the bridge, they have only modest gaps between the first and second one-electron oxidation/reduction potential(s).^{13–16} We have proposed an explanation of this fact.¹³ A recent review on the topic of long distance intervalence electron transfer also drew attention to this phenomenon,¹⁸ but it has escaped the notice of many workers who experiment with dinuclear systems. Another unusual aspect of the present work is the application of TDDFT to large odd-electron systems. It is probably of fundamental interest to porphyrin chemists, and indeed more widely, to test the modeling of these unique delocalized free radicals against the experimental results.

To our knowledge, there have not been any similar theoretical studies of reduced or oxidized delocalized dinuclear porphyrin systems. There have been many theoretical studies of spectra of various oxidation states of *mononuclear* porphyrins, metalloporphyrins, and their phthalocyanine analogues, and we refer readers to the studies of Mack and Stillman.¹⁹ In the current work, we did not prepare the corresponding anions and cations of the mononuclear zinc porphyrin precursors, so we did not attempt to compute their spectra. In our initial spectroelectrochemical studies of the oep systems, we reported the electronic spectrum of [Ni(oep-C₄-Ph)]⁻.¹³ This species, which is actually at the same oxidation level as the *dianions* of the dinuclear systems, shows a symmetrical absorption band at 11 100 cm⁻¹, but this band is far less intense than that found in the same region for the dimers. Regarding conjugated dinuclear systems, Kobayashi et al. studied both experimentally and theoretically the reduced states of planar β,β -fused dinuclear bis(*phthalocyanines*),²⁰ but these systems are rather different from our linearly conjugated *meso-meso* linked diporphyrins.

In the present study, we included phenyl substituents at the lateral and terminal *meso* positions, to mimic better the electronic distribution within the porphyrin rings, i.e., structure **4** as a model of **3**. This is the first set of calculations performed on alkyne-linked *triaryl*porphyrins. The *tert*-butyl substituents are expected to have minimal impact on the electronic structures, while the triphenyl substitution pattern may be important for obtaining better energy predictions. Our results show that these methods are actually rather successful in predicting the profiles of the absorption spectra in the lower energy region, but are less successful in the Soret region. The results indicate that the radical anion and cation are described well by a fully delocalized representation (Class III description) and that our previous qualitative picture of inter-porphyrin conjugation gains strong support from the theoretical treatment.

Computational Methods

Theoretical ab initio calculations of electronic transitions were performed with DFT as implemented in the Gaussian 03 code.²¹ The DFT model consisted of Becke Three Parameter Hybrid Functionals²² for the exchange with the correlation functional of Lee, Yang, and Parr²³ formalized as the B3LYP hybrid functional. Optimized geometric structures and properties were obtained by using a triple- ζ split valence basis set for the linear combination of three contracted Gaussian functions for each orbital type specified as the 6-311G basis set. For the series of butadiyne-bridged diporphyrins investigated in this work, we used six primitive s-shell functions for hydrogen and three sp-shells with three, one, and one primitives to describe carbon and nitrogen using the McLean–Chandler²⁴ basis set. The atomic orbitals of zinc were conveyed by using all electron pure Cartesian d functions as described by Wachters and Hay²⁵ with the scaling factors of Raghavachari and Trucks.²⁶

Restricted closed shell calculations were performed for molecular species with singlet spin multiplicity (neutral and dianion), while unrestricted open-shell calculations were performed for those with a doublet multiplicity (anion and cation). Starting structures were optimized at a semiempirical level before refinement to a B3LYP/6-311G geometry. Calculations of excited states were performed by using the optimized geometry of the refined structures, using the time-dependent (TD) extension of DFT as implemented in the Gaussian code. The output from the TDDFT calculations is presented as unbroadened line spectra of electronic transitions in the 30000–3000 cm⁻¹ region. To cover this full region, 120 excited states were included in the computations.

Multiple supercomputing facilities were utilized in this work; computer resource usage for the excited-state calculations for a butadiyne-bridged diporphyrin was dependent on several factors. Consideration must be given to computer hardware, quantum chemical algorithms, size of basis set, and spin multiplicity. For example, the neutral (singlet) oxidation state required 320 CPU hours over 8 processors with 9 Gb of shared memory for Gaussian 98, Revision A.7, operating on an SGI Origin 3000 [CPUs 124 × MIPS R14000A (600 MHz)]. On the other hand, the anionic (doublet) oxidation state required 288 CPU hours over 8 processors with 9 Gb of shared memory for Gaussian 03, Revision B.05 operating on an SGI Altix 3700 [CPUs 64 × Intel Itanium 2 (1.5 GHz)]. A typical calculation performed on an HP AlphaServer SC45 was on a single node [CPUs 4 × Alpha-EV68 (1 GHz)] and had similar resource demand.

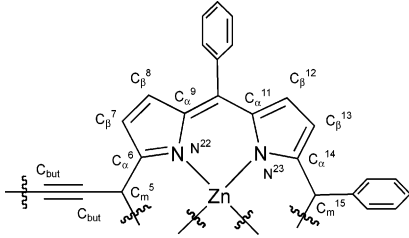
Experimental gas-phase absorption spectra are unavailable for these butadiyne-bridged diporphyrins. The observed spectra were recorded for neutral **3** in dichloromethane solution, with and without electrolyte (0.5 M tetrabutylammonium hexafluorophosphate, TBAPF₆). Our spectra of the oxidized and reduced states were obtained by low-temperature (220–233 K) in situ spectroelectrochemical measurements in an optically transparent thin layer electrochemical (OTTLE) cell, as described previously.¹⁴ For consistency, the “observed” spectra for all four oxidation states that are depicted in this work are those obtained in the presence of TBAPF₆. It is very difficult to obtain accurate molar absorptivities under our low-temperature conditions, especially as the small electrochemical gaps between the first and second one-electron reductions/oxidations do not allow us to obtain pure samples of the monoradicals. They are always contaminated with the neutral and dianionic/dicationic states within the limits of the Nernstian comproportionation constants. Therefore, the absorbance axes for the observed spectra are depicted in arbitrary absorbance units and are not normalized.

Results and Discussion

Geometries. The optimized geometries for all four oxidation states of **4** were obtained as described in Computational Methods section above. As expected, the resulting structures predict that the porphyrin rings are virtually coplanar, and therefore the molecules are centrosymmetric (point group D_{2h}). The largest distortion from planarity is for the neutral state, but this is still less than 10°. It has proved to be very difficult to obtain good experimental evidence for the favored inter-porphyrin angle in alkyne-linked diporphyrins. There is no X-ray crystal structure for a “simple” diporphyrin of this type, the known examples having additional intervening groups²⁷ or more exotic diyne substituents in the terminal *meso* positions.^{4c} The solution structures have been probed by various spectroscopic methods, and it seems clear that the statistically favored angle is near 0°, but that conformational freedom certainly still exists.^{4a,d,5b,28} Thus there will be an additional source of spectral broadening that cannot be accounted for in the spectral predictions based only on the optimized gas-phase structure. However, our earlier calculations suggested that the energy does not rise greatly until porphyrin interplanar angles of at least 30° are reached, so this factor is not expected to invalidate the major conclusions from the calculations. The dihedral angles between the porphyrin and phenyl substituent planes are, as expected, close to 90°.

The predicted bond lengths are shown in Table 1. The largest differences among the four oxidation states relate to the region of the butadiyne bridge. Notably, the bond alternation in the $C_{meso}-C\equiv C-C\equiv C-C_{meso}$ fragment is greatest in the neutral species, and a more “cumulenic” pattern applies for the other

TABLE 1: Selected Calculated Bond Lengths (Å) for the Four Oxidation States of the Butadiyne-Bridged Diporphyrin **4**



bond	bond length (Å)			
	cation	neutral	anion	dianion
$C_{but}-C_{but}'$	1.338	1.354	1.344	1.332
$C_{but}\equiv C_{but}$	1.231	1.222	1.231	1.242
$C_{but}-C_m^5$	1.398	1.418	1.402	1.385
$C_m^5-C_\alpha^6$	1.426	1.415	1.427	1.440
$C_\alpha^6-C_\beta^7$	1.444	1.446	1.439	1.433
$C_\beta^7-C_\beta^8$	1.364	1.363	1.370	1.376
$C_\beta^8-C_\alpha^9$	1.448	1.449	1.441	1.434
$C_\alpha^9-C_m^{10}$	1.398	1.401	1.406	1.410
$C_m^{10}-C_\alpha^{11}$	1.416	1.407	1.401	1.397
$C_\alpha^{11}-C_\beta^{12}$	1.445	1.448	1.445	1.442
$C_\beta^{12}-C_\alpha^{13}$	1.365	1.364	1.367	1.367
$C_\beta^{13}-C_\alpha^{14}$	1.445	1.448	1.449	1.451
$C_\alpha^{14}-C_m^{15}$	1.407	1.405	1.408	1.413
$C_\alpha^6-N^{22}$	1.373	1.381	1.381	1.380
$C_\alpha^9-N^{22}$	1.400	1.395	1.399	1.404
$C_\alpha^{11}-N^{23}$	1.384	1.388	1.398	1.406
$C_\alpha^{14}-N^{23}$	1.391	1.390	1.387	1.386
$N^{22}-Zn$	2.056	2.050	2.055	2.061
$N^{23}-Zn$	2.049	2.048	2.052	2.059

three states. The distance between the *meso* carbons of the two rings across the bridge diminishes in the order neutral > anion > cation > dianion, although the changes are modest, from 6.5848 to 6.6349 Å. These effects are expected when the orbital occupancies are considered (see below), and have consequences for discussions of the electrochemical “mixed-valence voltammetric splitting”, as noted in the Introduction.

Orbitals. In our previous discussions of the electronic structures of conjugated diporphyrins, we concentrated on the eight frontier orbitals that are derived from interactions of the four “Gouterman orbitals” of each porphyrin across the butadiyne (or other π -bonding) bridge.^{13,15} This set of orbitals is described conveniently by the gerade and ungerade combinations of so-called “x” orbitals (derived ultimately from the a_{2u} orbitals of a D_{4h} metalloporphyrin) and the “y” orbitals (from a_{1u}). The latter have nodes at the *meso* carbons, so undergo minimal interaction across the bridge. The symmetry labels are assigned on the basis of the molecule lying in the xy plane with the x axis along the C_4 unit. Since we are comparing four different oxidation states with appropriate orbital occupancies in this manifold, the descriptors HOMO, LUMO, etc. may be confusing and cumbersome, as the definition of “HOMO” etc. must be annotated separately for each oxidation state. Thus we will refer to the eight key orbitals for all four oxidation states by the x/y labels for the neutral species, as depicted in the second column in Figure 1, which shows the eigenvalues for the orbitals of all four oxidation levels, as derived from the TDDFT calculations.

For each species, the x,x^* orbitals that interact strongly via the bridge π orbitals are shown in the center, flanked by the almost degenerate y,y^* pairs. The shapes of the orbitals are shown for the neutral state in Figure 2, together with the orbital numbering from the calculations and the symmetry labels derived under the D_{2h} point group. These eight frontier orbitals are numbered 318–325 from the calculations, and the configu-

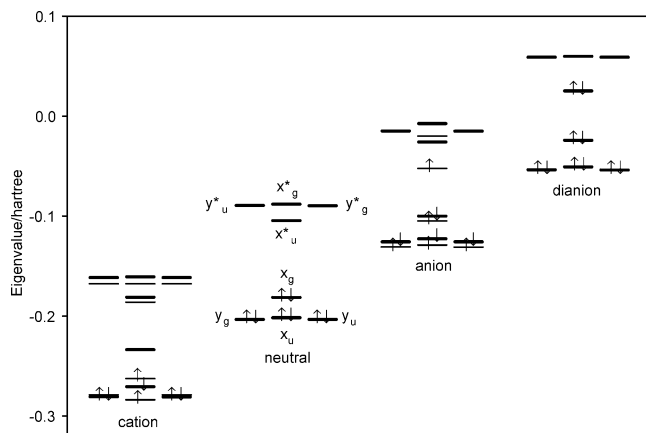


Figure 1. Calculated eigenvalues for the eight frontier orbitals of the four oxidation states of the butadiyne-bridged diporphyrin **4**. The x/y symmetry labels are attached for the neutral species, and the orbitals are arranged similarly for the other three oxidation states. For the radical cation and anion, the α and β levels are shown in light and bold, respectively.

rations that give rise to the excited states relevant to the visible to near-IR absorption bands are composed almost exclusively of these orbitals. In the tables listing the configurations contributing to the excited states (see below), both the numbers and pictorial labels (x , y , etc.) are included for the eight primary orbitals, while numbers alone are used for lower and higher orbitals. Similar orbital diagrams have been reported by others for comparable ethyne- and butadiyne-linked neutral diporphyrins, so we will not retrace the ground already covered well in those papers.^{10,11} The relative eigenvalues of the upper and lower frontier orbitals for the four oxidation states and indeed for the α and β electrons of the cation and anion differ subtly. However, in all but the cation (α electron levels), the y_u , y_g pair lies just below the x_u level. For the odd-electron systems, the α and β eigenvalues differ considerably in energy, and are shown in Figure 1 as light and bold lines, respectively. The α -spin singly occupied molecular orbitals (SOMOs) for the radicals are the x_g (cation) and x_u^* (anion) levels.

Excited States and Visible to Near-IR Electronic Absorption Spectra. Calculations of the lowest 120 excited states of all four oxidation levels were carried out with TDDFT. This generated a formidable amount of data, and most of the states and corresponding energy predictions are presented only in the Supporting Information. In Tables 2–5, the one-electron transitions contributing to the excited states of the neutral, cation, anion, and dianion, respectively, are listed in truncated form. Only those states giving rise to spin-allowed excitations having $f \geq 0.01$, and for the radicals, only those with predicted wavelengths >450 nm, are listed. In our discussions, we will concentrate on transitions derived mainly from the eight key orbitals. Interested readers may consult the more extensive tables in the Supporting Information. The excitation compositions and comparisons of calculated and observed spectra will be discussed together to avoid repetition.

Before presenting the results of the calculations, we review briefly the profiles of the absorption spectra exhibited by the four oxidation states, which are typical of those we have obtained for a variety of conjugated diporphyrins.^{13–16} The observed spectra are shown in Figure 3, overlaid with the predicted excitations represented in stick form. Note that the calculations are for the gas phase, while the observed spectra were recorded on solutions in dichloromethane containing 0.5 M TBAPF₆. The spectra of neutral butadiyne- or similar alkyne-bridged diporphyrins all show characteristic split B (Soret)

bands, the region consisting of several overlapping components, whose pattern of splitting, shoulders, and relative intensities depends on factors such as the nature of the porphyrin, the central metal ion, the presence of coordinating ligands, and temperature.^{13–16} In most cases, there is a rather prominent, red-shifted component near 500 nm. These now familiar spectra have been analyzed in various ways, both qualitative and theoretical. The degree of splitting of major bands in the B-region, or the width at half-maximum of the whole B-band spread have been used semiquantitatively for comparisons of inter-porphyrin coupling among related structures.^{4f,5b,10} Another feature noted for linearly conjugated diporphyrins of this type is a relative intensification and a red-shift of the lowest energy (Q) band (in comparison with monoporphyrins).

One-electron oxidation or reduction of **3** and similar diporphyrins causes remarkable changes to the electronic spectra that are analogous to those described for other delocalized radicals.²⁹ Notably, the longest wavelength band (described as “ ν_1 ” in our previous work, but here as $\tilde{\nu}_1$) is shifted strongly to the red and appears in the near to mid-IR region, at <5000 cm^{-1} .^{13–16} This is accompanied by another band (“ $\tilde{\nu}_2$ ”) near 10 000 cm^{-1} . This is accompanied by another band (“ $\tilde{\nu}_2$ ”) near 10 000 cm^{-1} , with an extinction coefficient about twice that of $\tilde{\nu}_1$. Both these bands for $[\mathbf{3}]^{+\bullet}$ and $[\mathbf{3}]^{-\bullet}$ are fairly narrow and asymmetric in shape, with widths at half-maximum ≤ 1000 cm^{-1} , and accompanied by shoulders on the blue side.¹⁶ This may be due to conformational inhomogeneity, as mentioned above, and/or to vibronic bands, but may also be a fundamental aspect of the band shape (particularly for $\tilde{\nu}_1$, see the final section below). For these radicals, the region between 12 000 and 19 000 cm^{-1} may contain numerous weak bands, but it is difficult, as noted in the Computational Methods section above, to quantify the contributions of the residual neutral or dianionic/dicationic states. It is especially difficult to deconvolute the bands of the radicals from those of the contaminants in the B-band region, but one clear conclusion is that the overall intensities of the bands in this region are diminished significantly relative to those of neutral **3**. Mack and Stillman used spectral subtraction to remove the contribution of neutral zinc phthalocyanine to the electronic spectra they recorded during photogeneration of the corresponding anion,^{19b} but this facility was unavailable to us. Last, for the dianion, an apparently simpler spectrum is observed, with one strong component ($\tilde{\nu}_1$) near 10 000 cm^{-1} and one major band with a very broad base and shoulders in the B-region. In the present case of the zinc complex $[\mathbf{3}]^{2-}$, the near-IR band is also very broad, with some shoulders. In most of our other examples of diporphyrin dianions, this band is smoothly shaped and narrower (e.g. see the spectra in ref 13). The near-IR band is very intense for most examples, with a molar absorptivity exceeding those of the B-bands of the neutral precursor.^{13,15} It is not clear why the band for $[\mathbf{3}]^{2-}$ has this shape and is so broad, but it may be due to aggregation, as the dianions of the analogous free base, dinickel(II), and bis[dichlorotin(IV)] derivatives all exhibit more “normal” shapes.³⁰ Clearly though, the overall profile of the spectrum of $[\mathbf{3}]^{2-}$ is consistent with expectations.

We begin our comparisons with the calculated excitations for the neutral molecule, given that all previous calculations on these diporphyrins have treated only this oxidation state. The excitation leading to the Q-band ($\tilde{\nu}_Q$) is composed of two degenerate y/y^* one-electron transitions and the classical HOMO-LUMO ($x_g \rightarrow x_u^*$) transition. The B-band region comprises several intense excitations involving mainly the eight key orbitals, but also including lower-lying occupied levels. In view of the large number of excitations in this region, it is not

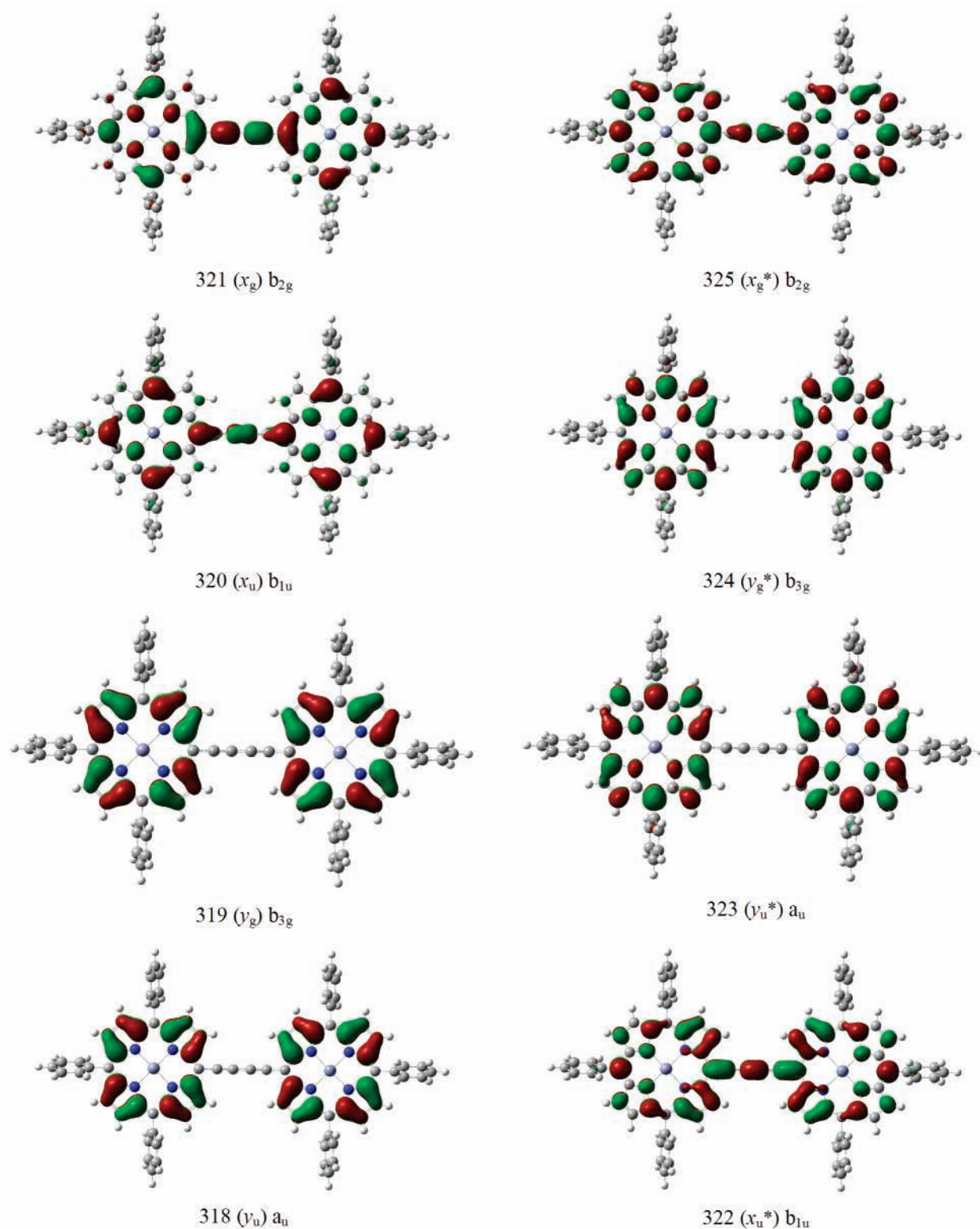


Figure 2. Frontier molecular orbitals of the neutral butadiyne-bridged diporphyrin **4**. The orbitals are labeled with the numbers from the calculations, the x/y formalism explained in the text, and the symmetry species under the D_{2h} point group.

possible to associate one-to-one the observed bands and calculated excitations. Clearly though, the characteristic “B-band splitting” said to be typical of alkyne-conjugated diporphyrins, is identifiable in these major transitions, e.g. excited states 8 and 13. In essence, a four-band spectrum is observed, and the calculations reproduce this pattern. At first sight from all the panels in Figure 3, the predicted *energies* do not correspond well, especially in the blue end of the spectrum. However, for

the major visible and near-IR bands of interest, whose positions can be readily associated with specific excitations in Tables 2–5, there may be a significant energy shift due to the medium. In electrolyte-free dichloromethane, the Q-band maximum for neutral **3** corresponds remarkably well: 14 760 (obsd), 14 900 cm^{-1} (calcd); $\Delta E = 0.017$ eV. There is a significant red-shift of the observed band maximum to 13 800 cm^{-1} in the electrolyte solution. One could speculate that a similar effect may apply

TABLE 2: TDDFT Calculated Excitation Energies, One-Electron Transitions, and Oscillator Strengths for Optical Transitions of Neutral Diporphyrin 4 in the Gas Phase ($\lambda > 400$ nm; $f > 0.01$)

excited state	orbital composition	coeff	excitation			oscillator strength
			eV	nm	cm ⁻¹	
1	318 (y _u) → 324 (y _g [*])	-0.142	1.85	670	14900	1.42
	319 (y _g) → 323 (y _u [*])	0.142				
	321 (x _g) → 322 (x _u [*])	0.638				
2	318 (y _u) → 325 (x _g [*])	0.172	2.10	590	17000	0.0179
	319 (y _g) → 322 (x _u [*])	-0.384				
	320 (x _u) → 324 (y _g [*])	0.111				
7	321 (x _g) → 323 (y _u [*])	0.565	2.53	490	20400	0.142
	318 (y _u) → 325 (x _g [*])	0.113				
	319 (y _g) → 322 (x _u [*])	0.457				
8	320 (x _u) → 324 (y _g [*])	-0.381	2.62	473	21100	0.660
	321 (x _g) → 323 (y _u [*])	0.334				
	318 (y _u) → 324 (y _g [*])	-0.318				
10	319 (y _g) → 323 (y _u [*])	0.320	2.73	454	22000	0.0260
	320 (x _u) → 325 (x _g [*])	0.511				
	321 (x _g) → 322 (x _u [*])	-0.126				
13	318 (y _u) → 325 (x _g [*])	0.498	3.08	402	24900	1.16
	319 (y _g) → 322 (x _u [*])	0.256				
	320 (x _u) → 324 (y _g [*])	0.421				
15	315 → 322 (x _u [*])	0.261	3.09	401	24900	0.255
	316 → 325 (x _g [*])	0.126				
	317 → 322 (x _u [*])	0.311				
15	318 (y _u) → 324 (y _g [*])	0.225	3.09	401	24900	0.255
	319 (y _g) → 323 (y _u [*])	-0.219				
	320 (x _u) → 325 (x _g [*])	0.372				
15	321 (x _g) → 326	-0.161	3.09	401	24900	0.255
	315 → 322 (x _u [*])	0.578				
	316 → 325 (x _g [*])	0.274				
15	317 → 322 (x _u [*])	-0.142	3.09	401	24900	0.255
	318 (y _u) → 324 (y _g [*])	-0.101				
	320 (x _u) → 325 (x _g [*])	-0.169				

for the other three oxidation states, but we have no evidence that this is the case. In Table 6, the calculated and observed wavenumbers of these bands are compared, and the correlation between these quantities is explored in Figure 4. There is a good correlation ($r = 0.993$), but whether this has any systematic significance is unclear. In the absence of independent confirmation of a ca. 1000 cm⁻¹ red-shift due to the electrolyte for the oxidized and reduced species, one can only wonder at this stage whether the agreement for the neutral species is uniquely close. It should be possible to prepare these oxidation states by chemical rather than electrochemical reactions, thus avoiding the presence of electrolyte, and the present results encourage us to do this in the future. However, the agreement for all these bands without “correcting” for a possible medium effect is nevertheless rather good, being less than 0.3 eV in the worst case.

The spectra of the cation and anion radicals can be treated equivalently, as their low-energy bands are expected to have analogous origins, due to particle-hole parity and the similar energy gaps in the upper and lower halves of the eight orbital manifold. We have explained these spectra by a crude approach using strictly single configuration excited states and the eight-orbital picture. In the more sophisticated TDDFT approach, many configurations contribute to the excited states in the visible to near-IR region, and many excited states lie within this energy band. This situation is exacerbated by the presence of the odd electron, so that separate transitions must be included for α and β electrons in all cases. The excited states of most interest are those giving rise to $\tilde{\nu}_1$ and $\tilde{\nu}_2$, calculated for [4]^{•+} to lie at 6 500 and 12 700 cm⁻¹, respectively, and for [4]^{•-} at 5 900 and 12 300 cm⁻¹. This slight red-shift of the anion band relative to the cation is observed in practice (3640 vs 4090 cm⁻¹), as are the relative intensities of $\tilde{\nu}_1$ and $\tilde{\nu}_2$. This extends also to the apparent slight difference in the intensity *ratio* of $\tilde{\nu}_1/\tilde{\nu}_2$, that for the anion being

TABLE 3: TDDFT Calculated Excitation Energies, One-Electron Transitions, and Oscillator Strengths for Optical Transitions of Diporphyrin Radical Cation [4]^{•+} in the Gas Phase ($\lambda > 450$ nm; $f > 0.01$)

excited state	orbital composition	coeff	excitation			oscillator strength
			eV	nm	cm ⁻¹	
3	321 α (x _g) → 322 α (x _u [*])	-0.346	0.805	1540	6490	0.709
	317 β → 322 β (x _u [*])	0.107				
	320 β (x _u) → 321 β (x _g)	0.868				
5	318 α (x _u) → 325 α (y _g [*])	-0.280	1.57	789	12700	1.23
	319 α (y _u) → 324 α (x _g [*])	0.199				
	320 α (y _g) → 323 α (y _u [*])	-0.200				
22	321 α (x _g) → 322 α (x _u [*])	0.882	2.04	607	16500	0.0764
	300 β → 321 β (x _g)	0.109				
	320 β (x _u) → 321 β (x _g)	0.150				
22	320 β (x _u) → 325 β (x _g [*])	0.203	2.04	607	16500	0.0764
	318 α (x _u) → 324 α (x _g [*])	0.163				
	320 α (y _g) → 322 α (x _u [*])	0.124				
25	321 α (x _g) → 323 α (y _u [*])	-0.523	2.10	592	16900	0.188
	293 β → 321 β (x _g)	0.102				
	302 β → 321 β (x _g)	0.137				
25	313 β → 321 β (x _g)	0.632	2.10	592	16900	0.188
	316 β → 321 β (x _g)	0.236				
	318 β (y _u) → 325 β (x _g [*])	-0.159				
38	319 β (y _g) → 322 β (x _u [*])	-0.360	2.32	535	18700	0.0366
	320 β (x _u) → 323 β (y _u [*])	-0.225				
	319 α (y _u) → 324 α (x _g [*])	-0.532				
38	320 α (y _g) → 323 α (y _u [*])	0.534	2.32	535	18700	0.0366
	321 α (x _g) → 322 α (x _u [*])	0.150				
	291 β → 321 β (x _g)	0.102				
42	300 β → 321 β (x _g)	0.175	2.54	488	20500	0.0622
	314 β → 321 β (x _g)	0.273				
	318 β (y _u) → 323 β (y _u [*])	-0.431				
42	319 β (y _g) → 324 β (y _g [*])	0.431	2.54	488	20500	0.0622
	320 α (y _g) → 322 α (x _u [*])	-0.482				
	321 α (x _g) → 323 α (y _u [*])	-0.126				
42	318 β (y _u) → 325 β (x _g [*])	-0.116	2.54	488	20500	0.0622
	319 β (y _g) → 322 β (x _u [*])	-0.525				
	320 β (x _u) → 323 β (y _u [*])	0.659				
43	318 α (x _u) → 324 α (x _g [*])	-0.281	2.64	470	21300	0.435
	319 α (y _u) → 325 α (y _g [*])	0.650				
	320 α (y _g) → 322 α (x _u [*])	0.408				
43	320 α (y _g) → 326 α	-0.101	2.64	470	21300	0.435
	321 α (x _g) → 323 α (y _u [*])	-0.327				
	319 β (y _g) → 322 β (x _u [*])	0.171				
43	320 β (x _u) → 323 β (y _u [*])	0.403	2.64	470	21300	0.435
	317 α → 322 α (x _u [*])	-0.243				
	318 α (x _u) → 325 α (y _g [*])	0.585				
45	319 α (y _u) → 324 α (x _g [*])	-0.226	2.66	466	21500	0.0652
	320 α (y _g) → 323 α (y _u [*])	0.232				
	321 α (x _g) → 322 α (x _u [*])	0.100				
45	321 α (x _g) → 326 α	-0.130	2.66	466	21500	0.0652
	291 β → 321 β (x _g)	-0.140				
	317 β → 322 β (x _u [*])	0.177				
45	318 β (y _u) → 323 β (y _u [*])	0.334	2.66	466	21500	0.0652
	319 β (y _g) → 324 β (y _g [*])	-0.332				
	320 β (x _u) → 325 β (x _g [*])	0.383				
45	318 α (x _u) → 324 α (x _g [*])	0.583	2.66	466	21500	0.0652
	319 α (y _u) → 325 α (y _g [*])	0.524				
	320 α (y _g) → 322 α (x _u [*])	0.108				
45	321 α (x _g) → 323 α (y _u [*])	0.364	2.66	466	21500	0.0652
	318 β (y _u) → 325 β (x _g [*])	0.224				
	319 β (y _g) → 322 β (x _u [*])	-0.389				

higher than for the cation, both theoretically and experimentally. For the reasons noted above, it is impossible to analyze the higher energy end of the spectrum with any certainty.

The orbital situation giving rise to the $\tilde{\nu}_1$ excitation is analogous to that described by Halasinski et al. in their analysis of the absorption spectra of arylene radicals by TDDFT methods, and our treatment draws on those ideas.³¹ The radical transitions involve a superposition of two or more configurations that must be taken together to describe the total one-electron excitations. The radical cation α excitation (x_g α → x_u^{*} α) is the analogue of the HOMO-LUMO transition in the neutral molecule, but the total excitation has contributions in both α and β electron

TABLE 4: TDDFT Calculated Excitation Energies, One-Electron Transitions, and Oscillator Strengths for Optical Transitions of Diporphyrin Radical Anion [4]⁻ in the Gas Phase ($\lambda > 450$ nm; $f > 0.01$)

excited state	orbital composition	coeff	excitation			oscillator strength
			eV	nm	cm ⁻¹	
3	322 α (x_u^*) \rightarrow 323 α (y_u^*)	0.833	0.731	1700	5900	0.652
	321 β (x_g) \rightarrow 322 β (x_u^*)	0.367				
4	320 α (x_u) \rightarrow 323 α (y_u^*)	0.203	1.53	813	12300	1.220
	322 α (x_u^*) \rightarrow 323 α (y_u^*)	-0.143				
	322 α (x_u^*) \rightarrow 327 α	-0.151				
	318 β (y_u) \rightarrow 324 β (x_g^*)	0.161				
	319 β (y_g) \rightarrow 323 β (y_u^*)	0.162				
10	320 β (x_u) \rightarrow 325 β (y_g^*)	-0.274				
	321 β (x_g) \rightarrow 322 β (x_u^*)	0.892				
	320 α (x_u) \rightarrow 324 α (y_g^*)	0.112	2.04	608	16400	0.0123
	321 α (x_g) \rightarrow 325 α (x_g^*)	0.634				
	318 β (y_u) \rightarrow 325 β (y_g^*)	0.302				
13	319 β (y_g) \rightarrow 322 β (x_u^*)	0.644				
	321 β (x_g) \rightarrow 323 β (y_u^*)	-0.319				
	318 α (y_u) \rightarrow 325 α (x_g^*)	-0.444	2.13	581	17200	0.155
	319 α (y_g) \rightarrow 324 α (y_g^*)	0.449				
	320 α (x_u) \rightarrow 323 α (y_u^*)	-0.217				
15	322 α (x_u^*) \rightarrow 327 α	0.478				
	318 β (y_u) \rightarrow 324 β (x_g^*)	-0.364				
	319 β (y_g) \rightarrow 323 β (y_u^*)	-0.365				
	320 β (x_u) \rightarrow 325 β (y_g^*)	0.237				
	321 β (x_g) \rightarrow 322 β (x_u^*)	0.220				
25	319 α (y_g) \rightarrow 323 α (y_u^*)	0.581	2.20	563	17800	0.121
	321 α (x_g) \rightarrow 325 α (x_g^*)	0.334				
	318 β (y_u) \rightarrow 325 β (y_g^*)	-0.174				
	319 β (y_g) \rightarrow 322 β (x_u^*)	-0.462				
	320 β (x_u) \rightarrow 324 β (x_g^*)	-0.243				
34	321 β (x_g) \rightarrow 323 β (y_u^*)	-0.487				
	322 α (x_u^*) \rightarrow 332 α	0.991	2.37	523	19100	0.0290
	318 α (y_u) \rightarrow 325 α (x_g^*)	0.369	2.60	476	21000	0.556
	319 α (y_g) \rightarrow 324 α (y_g^*)	-0.374				
	320 α (x_u) \rightarrow 323 α (y_u^*)	0.294				
36	321 α (x_g) \rightarrow 326 α	-0.129				
	317 β \rightarrow 322 β (x_u^*)	-0.253				
	318 β (y_u) \rightarrow 324 β (x_g^*)	-0.262				
	319 β (y_g) \rightarrow 323 β (y_u^*)	-0.269				
	320 β (x_u) \rightarrow 325 β (y_g^*)	0.584				
36	321 β (x_g) \rightarrow 326 β	0.191				
	317 α \rightarrow 325 α (x_g^*)	0.108	2.61	474	21000	0.0519
	319 α (y_g) \rightarrow 323 α (y_u^*)	0.533				
	320 α (x_u) \rightarrow 324 α (y_g^*)	0.632				
	321 α (x_g) \rightarrow 325 α (x_g^*)	-0.322				
36	318 β (y_u) \rightarrow 325 β (y_g^*)	-0.163				
	319 β (y_g) \rightarrow 322 β (x_u^*)	0.390				

spaces. One transition in the β space for the cation is from doubly occupied $x_u \beta$ to the SOMO. Another β transition from a lower orbital (317, the highest x_g orbital below the eight key orbitals) also contributes to the excitation. The analogous picture for the radical anion in which orbital 322 α (x_u^*) is the SOMO is that the total excitation giving rise to $\tilde{\nu}_1$ is a superposition of just two configurations, namely $x_u^* \rightarrow x_g^*$ (α) and $x_g \rightarrow x_u^*$ (β). The band $\tilde{\nu}_2$ for both the cation and anion is a complex superposition of configurations involving not only α and β transitions among x levels, including the SOMOs, but also the y and y^* orbitals.

The situation for the dianion is remarkably simple, in that the calculations predict one very intense absorption at 9800 cm⁻¹ comprising a single configuration, namely the ‘‘upper-storey’’, $x_u^* \rightarrow x_g^*$ transition. The very high oscillator strength predicted for this excitation (2.487) is larger even than those predicted for the B-bands of the neutral diporphyrin. This intensity expectation is apparently not met, although as noted above, we have not attempted to convert the oscillator strengths into molar absorptivities. The signature spectral feature of these conjugated diporphyrin dianions is this strong band near 10 000 cm⁻¹, and the calculations give a clear indication of its origin.

TABLE 5: TDDFT Calculated Excitation Energies, One-Electron Transitions, and Oscillator Strengths for Optical Transitions of Diporphyrin Dianion [4]²⁻ in the Gas Phase ($\lambda > 400$ nm; $f > 0.01$)

excited state	orbital composition	coeff	excitation			oscillator strength
			eV	nm	cm ⁻¹	
3	322 (x_u^*) \rightarrow 325 (x_g^*)	0.493	1.21	1021	9790	2.487
10	321 (x_g) \rightarrow 323 (y_u^*)	-0.101	1.88	659	15200	0.0382
	322 (x_u^*) \rightarrow 329	0.670				
11	322 (x_u^*) \rightarrow 331	0.186				
	322 (x_u^*) \rightarrow 333	0.691	1.89	655	15300	0.0633
18	319 (y_g) \rightarrow 325 (x_g^*)	-0.182	2.01	615	16300	0.210
	321 (x_g) \rightarrow 323 (y_u^*)	0.650				
20	318 (y_u) \rightarrow 323 (y_u^*)	0.154	2.20	563	17800	0.0185
	319 (y_g) \rightarrow 324 (y_g^*)	0.159				
22	320 (x_u) \rightarrow 325 (x_g^*)	-0.103				
	322 (x_u^*) \rightarrow 339	0.652				
	318 (y_u) \rightarrow 323 (y_u^*)	0.305	2.58	481	20800	0.516
	319 (y_g) \rightarrow 324 (y_g^*)	0.307				
	320 (x_u) \rightarrow 325 (x_g^*)	0.542				
23	319 (y_g) \rightarrow 325 (x_g^*)	-0.426	2.63	472	21200	0.0123
	320 (x_u) \rightarrow 324 (y_g^*)	0.555				
27	318 (y_u) \rightarrow 323 (y_u^*)	0.112	2.92	425	23500	0.219
	319 (y_g) \rightarrow 324 (y_g^*)	0.135				
	320 (x_u) \rightarrow 325 (x_g^*)	-0.223				
29	321 (x_g) (x_g) \rightarrow 326	0.628				
	319 (y_g) \rightarrow 325 (x_g^*)	0.486	3.01	412	24300	0.994
	320 (x_u) \rightarrow 324 (y_g^*)	0.375				
	322 (x_u^*) \rightarrow 356	0.134				

Relation to Previous Descriptions. In our previous simplistic discussions of the spectra of these species, we relied upon a model of single configuration, one-electron excitations with inclusion of an empirical ‘‘electron-pair correlation’’ term for doubly occupied to unoccupied orbital transitions.^{13,15} We argued that the degree of inter-porphyrin coupling could be equated simply to the x_u/x_g and x_u^*/x_g^* orbital energy gaps of the neutral compound. These were (for convenience) assumed to be identical when we had data only for the anion. TDDFT calculates these gaps to be 4400 and 3640 cm⁻¹, respectively. We then made the connection to the oxidized and reduced states, by postulating that the lower and upper energy gaps could be determined experimentally from the wavenumbers of $\tilde{\nu}_1$ for the cation and anion, respectively. In this naive picture, the transitions $x_u \rightarrow x_g$ for the former and $x_u^* \rightarrow x_g^*$ for the latter are representative of this separation, since only singly occupied or unoccupied orbitals are involved, and electron correlation can be ignored. Remarkably, the experimental wavenumbers so determined are 4090 and 3640 cm⁻¹, respectively. Thus the postulate is rather well supported, despite all the uncertainties and simplifications. It may be interesting to see if this picture can be confirmed by calculations on diporphyrins having conjugated bridges that are more complex than the simple C₄ unit.

In our previous work, and in the Introduction, we alluded to the fact that [3]⁺ and [3]⁻ may be regarded as organic mixed-valence systems. Originally, we labeled $\tilde{\nu}_1$ as an intervalence charge transfer (IVCT) band, but noted its exceptionally high intensity and narrow line width. It is apparent that these radical ions are better treated simply as completely delocalized, i.e., Class III in the Robin and Day classification.³² Therefore the term ‘‘IVCT band’’ is not really suitable, as the barrier to intramolecular charge transfer has vanished and the low-energy optical band is simply a $\pi \rightarrow \pi$ transition of the supermolecule. This situation, and particularly compounds on the Class II/III borderline, was explored descriptively in a review by Nelson,³³ and in an extensive mathematical analysis by Brunschwig et al.³⁴ A key point about the optical absorption bands of Class III ions is that the band should be non-Gaussian in shape, with a steep cutoff on the red side. The maximum of this band is

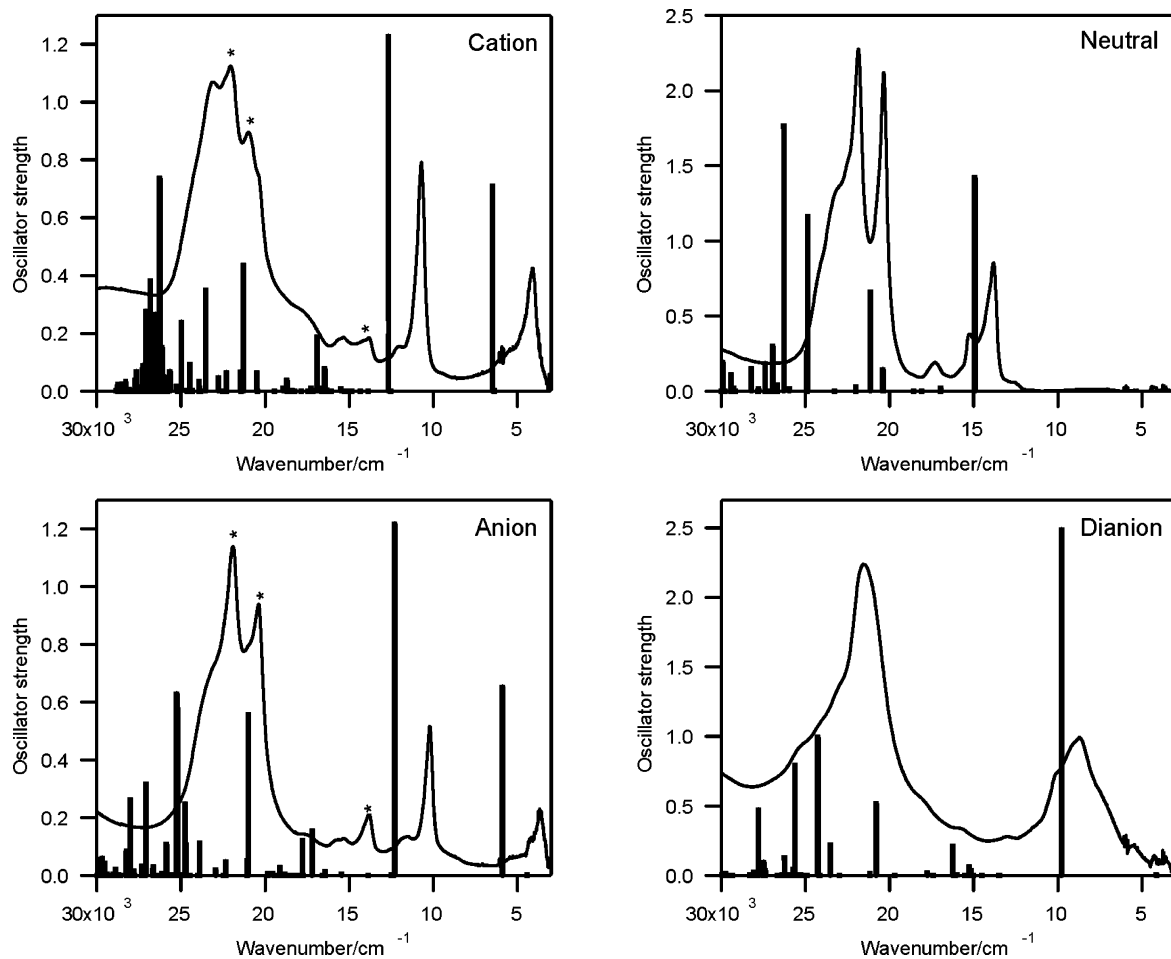


Figure 3. Calculated excitations of **4** (vertical lines) and observed absorption spectra (in 0.5 M TBAPF₆ in CH₂Cl₂) of **3** in the four oxidation states. The y axes for the experimental spectra are in arbitrary absorbance units, and are not normalized between panels. The experimental spectra have been artificially smoothed in the region 3000–7000 cm⁻¹, by editing out spikes due to overtones of the solvent and hence poor baseline correction. Residual neutral **3** is responsible for some of the intensity of the peaks marked with an asterisk (see text for explanation).

TABLE 6: Observed (for **3, in Dichloromethane with 0.5 M TBAPF₆) and Calculated (for **4**) Wavenumbers (cm⁻¹) for the Visible to Near-IR Absorption Bands of the Four Oxidation States**

ox. state	$\tilde{\nu}_1^a$		$\tilde{\nu}_2^a$		$\tilde{\nu}_Q^a$	
	obsd	calcd	obsd	calcd	obsd ^b	calcd
1+	4090	6500	10710	12700		
0					13800	14900
1-	3640	5900	10210	12300		
2-	8690	9800				

^a The terms $\tilde{\nu}_1$, $\tilde{\nu}_2$, and $\tilde{\nu}_Q$ are described in the text. ^b In CH₂Cl₂ without electrolyte, $\tilde{\nu}_Q(\text{obsd}) = 14\,760\text{ cm}^{-1}$.

related directly to the electronic coupling between the halves of the molecule, H_{AB} , by the relationship $\tilde{\nu}_{\text{max}} = 2H_{AB}$. This is conceptually the same as our model of $\tilde{\nu}_1$ for [3]⁺ representing the x_u/x_g splitting and that for [3]⁻, the x_u^*/x_g^* splitting. The profiles for $\tilde{\nu}_1$ are clearly highly asymmetric, having a steep slope on the red edge. However, our observations of this aspect are inadequate because this region is so close to the roll-off of our instrument at 3125 cm⁻¹, and accurate recording is made more difficult by the strong solvent overtones. Further clarification of these points must await examination of the radical cations and anions of these or similar molecules prepared by chemical means and using an instrument that can scan the full extent of the peak with equal sensitivity.

We referred above to our argument about the use of the voltammetric splitting between the first and second one-electron

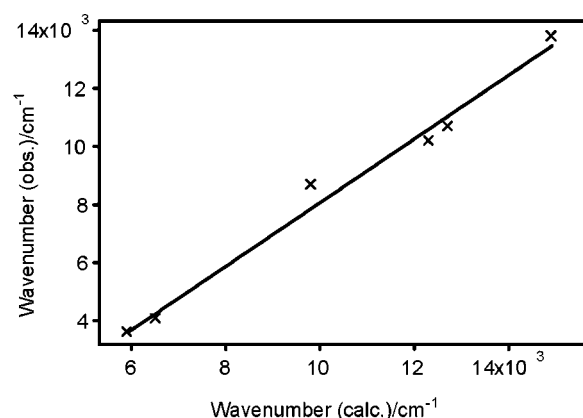


Figure 4. Observed (for **3**, in dichloromethane with 0.5 M TBAPF₆) vs calculated (for **4**) wavenumbers (cm⁻¹) for the visible to near-IR absorption bands of the four oxidation states of butadiyne-bridged diporphyrins.

per molecule reductions/oxidations as a measure of intradimer coupling. As we stated in our earlier papers, the fact that the splitting is modest (50–100 mV, for example) does not necessarily mean that the interaction between the porphyrins is small, nor does a large splitting necessarily mean the opposite. We refer the reader to the discussion by Arnold, Heath, and James¹³ for a fuller explanation of this topic. The key feature that is very obvious from Figure 1 is that intradimer “bonding” in the dianionic state is very strong, as the pairing of electrons

in the unique, low-lying x_u^* orbital shows. This is precisely the point that we made in ref 13. The x_u^* orbital, now doubly occupied, is of the “cumulenic” type, with enhanced bonding between the *meso* carbons and the carbon atoms 1 and 4 of the bridge, and a formal π bond between carbon atoms 2 and 3 (see Figure 2). Therefore a voltammetric splitting of only 100 mV is quite congruent with a large interaction energy of some 4000 cm^{-1} , and a completely delocalized situation. The bonding interaction introduced in the monanion/cation by the presence of two electrons in this orbital must be taken into account in the comproportionation energy. As advocated by Launay, “this use of (voltammetric) wave splitting is very qualitative and should be discouraged”.¹⁸ The fact that these dianions are EPR silent is further confirmation of the double occupation of the unique x_u^* orbital.

Conclusions

The availability of spectra for **3** in four oxidation states, including the odd-electron cation and anion, has enabled us to test rigorously the performance of TDDFT calculations in predicting excitation energies in these large aromatic systems. This approach has proved to be rather successful, as the salient features of the visible to near-IR spectra of all four species were modeled accurately. Despite some uncertainties in comparisons, due to medium effects, the gas-phase calculations have reproduced key features. (i) The energy calculated for the Q-band of the neutral species agrees within 200 cm^{-1} of that observed for **[3]**⁰ measured in dichloromethane in the absence of electrolyte. (ii) The characteristic near-IR bands for **[3]**⁺ and **[3]**⁻ are reproduced well in terms of relative intensities and energy separation $\tilde{\nu}_2 - \tilde{\nu}_1$ (obsd 6620, calcd 6650 cm^{-1} for the cation; 6570, 6400 cm^{-1} for the anion). (iii) The slight red-shift of $\tilde{\nu}_1$ for the anion relative to the cation is predicted (obsd 450, calcd 600 cm^{-1}). (iv) The strong near-IR band for the dianion is assigned to a single configuration, one-electron excitation, from a unique doubly filled x -aligned orbital.

There are still some aspects that are not well predicted. The profiles of the spectral bands in the blue end of the visible spectra of all the oxidation states are not well reproduced in terms of absolute energies, although we cannot obtain clear spectra of pure **[3]**⁺ and **[3]**⁻ due to the rather modest comproportionation constants. Due to the large number of atoms in the molecules, it is expected that the predictions involving the core electrons will be limited in accuracy due to basis set limitations. The B3LYP/6-311G model has successfully been utilized for polycyclic aromatic systems, notably to describe low-lying excited states, including those of delocalized odd-electron cations and anions.³¹ For high-energy excited states (e.g. B-bands of porphyrin macrocycles) or long-range charge-transfer bands, care must be taken as substantial errors can arise from TDDFT calculations.³⁵ This model has apparently not yet been applied to simple porphyrin monomers. The characteristic splitting of the B-band into one major red-shifted component and a manifold of overlapping absorptions is clear, but the intensity ascribed to the former is too low. Moreover, the splitting exhibited in the B-region for **[3]**⁰ is much less than the calculations predict. The oscillator strength calculated for the near-IR band for **[4]**²⁻ appears to be out of proportion to what is observed for **[3]**²⁻, although we certainly have seen similar very intense bands in spectra of our bis[Ni(oep)] systems (see Figure 4 in ref 15).

Butadiyne-linked conjugated diporphyrins are still attracting attention in the literature, most recently in the field of two-photon absorption.^{8e-g,11} The unique ground and excited state

optical properties afforded by the synthetically straightforward linking of two porphyrins by a C₄ bridge continue to challenge our understanding of porphyrin and other large delocalized structures. Our contribution has been to extend these discussions over three additional oxidation states and thus to test the applicability of theoretical treatment more stringently. The TDDFT approach has, we submit, done rather well in this regard, and we hope to stimulate continuation of theoretical and spectroscopic studies of these fascinating structures, for the sake of both fundamental and practical knowledge.

Acknowledgment. The authors thank Dr. Geoffrey Will for supporting the involvement of G.J.W. in this work, and acknowledge Dr. Anthony Rasmussen (QUT), Dr. Martin Nicholls (The University of Queensland), and Dr. Rika Kobayashi (Australian Partnership for Advanced Computing, APAC) for their assistance with their respective High Performance Computing Facilities. This work was supported financially by awards under the Queensland Parallel Supercomputing Foundation (QPSF) and APAC. G.J.W. acknowledges the financial support of the QUT PRA scholarship scheme. D.P.A. thanks Dr. Graham Heath, The Australian National University, for many helpful discussions on the electronic structures of these molecules, and for the provision of instrumental facilities for the experimental work.

Supporting Information Available: Supplementary Tables 1–4 providing the full list of excitations for the 120 lowest excited states for the four oxidation states of **4**. This material is available free of charge via the Internet at <http://pubs.acs.org>.

References and Notes

- (1) For example: (a) Holten, D.; Bocian, D. F.; Lindsey, J. S. *Acc. Chem. Res.* **2002**, *35*, 57. (b) Fukuzumi, S.; Ohkubo, K.; E, W.; Ou, Z.; Shao, J.; Kadish, K. M.; Hutchison, J. A.; Ghiggino, K. P.; Santic, P. J.; Crossley, M. J. *J. Am. Chem. Soc.* **2003**, *125*, 14984. (c) Kim, D.; Osuka, A. *Acc. Chem. Res.* **2004**, *37*, 735. (d) Matsuzaki, Y.; Nogami, A.; Iwaki, Y.; Ohta, N.; Yoshida, N.; Aratani, N.; Osuka, A.; Tanaka, K. *J. Phys. Chem. A* **2005**, *109*, 703.
- (2) (a) Blake, I. M.; Rees, L. H.; Claridge, T. D. W.; Anderson, H. L. *Angew. Chem., Int. Ed.* **2000**, *39*, 1818. (b) Tsuda, A.; Furuta, H.; Osuka, A. *J. Am. Chem. Soc.* **2001**, *123*, 10304. (c) Blake, I. M.; Krivokapic, A.; Katterle, M.; Anderson, H. L. *Chem. Commun.* **2002**, 1662. (d) Sendt, K.; Johnston, L. A.; Hough, W. A.; Crossley, M. J.; Hush, N. S.; Reimers, J. R. *J. Am. Chem. Soc.* **2002**, *124*, 9299. (e) Cho, H. S.; Jeong, D. H.; Cho, S.; Kim, D.; Matsuzaki, Y.; Tanaka, K.; Tsuda, A. *J. Am. Chem. Soc.* **2002**, *124*, 14642. (f) Bonifazi, D.; Scholl, M.; Song, F.; Echegoyen, L.; Accorsi, G.; Armaroli, N.; Diederich, F. *Angew. Chem., Int. Ed.* **2003**, *42*, 4966.
- (3) (a) Arnold, D. P.; Johnson, A. W.; Mahendran, M. *J. Chem. Soc., Perkin Trans. 1* **1978**, 366. (b) Arnold, D. P.; Nitschinsk, L. *J. Tetrahedron* **1992**, *48*, 8781.
- (4) (a) Anderson, H. L. *Inorg. Chem.* **1994**, *33*, 972. (b) O’Keefe, G. E.; Denton, G. J.; Harvey, E. J.; Phillips, R. T.; Friend, R. H.; Anderson, H. L. *J. Chem. Phys.* **1996**, *104*, 805. (c) Taylor, P. N.; Huuskonen, J.; Rumbles, G.; Aplin, R. T.; Williams, E.; Anderson, H. L. *Chem. Commun.* **1998**, 909. (d) Wilson, G. S.; Anderson, H. L. *Chem. Commun.* **1999**, 1539. (e) Anderson, H. L. *Chem. Commun.* **1999**, 2323. (f) Piet, J. J.; Taylor, P. N.; Anderson, H. L.; Osuka, A.; Warman, J. M. *J. Am. Chem. Soc.* **2000**, *122*, 1749. (g) Piet, J. J.; Taylor, P. N.; Wegewijs, B. R.; Anderson, H. L.; Osuka, A.; Warman, J. M. *J. Phys. Chem. B* **2001**, *105*, 97.
- (5) (a) Lin, V. S.-Y.; DiMugno, S. G.; Therien, M. J. *Science* **1994**, *264*, 1105. (b) Lin, V. S.-Y.; Therien, M. J. *Chem. Eur. J.* **1996**, *1*, 645. (c) Angiolillo, P. J.; Lin, V. S.-Y.; Vanderkooi, J. M.; Therien, M. J. *J. Am. Chem. Soc.* **1995**, *117*, 12514. (d) Kumble, R.; Palese, S.; Lin, V. S.-Y.; Therien, M. J.; Hochstrasser, R. M. *J. Am. Chem. Soc.* **1998**, *120*, 11489. (e) Angiolillo, P. J.; Susumu, K.; Uyeda, H. T.; Lin, V. S.-Y.; Shediach, R.; Therien, M. J. *Synth. Met.* **2001**, *116*, 247. (f) Susumu, K.; Therien, M. J. *J. Am. Chem. Soc.* **2002**, *124*, 8550. (g) Rubtsov, I. V.; Susumu, K.; Rubtsov, G. I.; Therien, M. J. *J. Am. Chem. Soc.* **2003**, *125*, 2687. (h) Ostrowski, J. C.; Susumu, K.; Robinson, M. R.; Therien, M. J.; Bazan, G. C. *Adv. Mater.* **2003**, *15*, 1296.
- (6) (a) Imahori, H.; Higuchi, H.; Matsuda, Y.; Itagaki, A.; Sakai, Y.; Ojima, J.; Sakata, Y. *Bull. Chem. Soc. Jpn.* **1994**, *67*, 2500. (b) Sugiura,

- K.-i.; Fujimoto, Y.; Sakata, Y. *Chem. Commun.* **2000**, 1105. (c) Susumu, K.; Maruyama, H.; Kobayashi, H.; Tanaka, K. *J. Mater. Chem.* **2001**, *11*, 2262. (d) Higuchi, H.; Maeda, T.; Miyabayashi, K.; Miyake, M.; Yamamoto, K. *Tetrahedron Lett.* **2002**, *43*, 3097. (e) Hayashi, N.; Naoe, A.; Miyabayashi, K.; Yamada, M.; Miyake, M.; Higuchi, H. *Tetrahedron Lett.* **2004**, *45*, 8215. (f) Nakamura, K.; Fujimoto, T.; Takara, S.; Sugiura, K.-i.; Miyasaka, H.; Ishii, T.; Yamashita, M.; Sakata, Y. *Chem. Lett.* **2003**, *32*, 694. (g) Kato, A.; Sugiura, K.-i.; Miyasaka, H.; Tanaka, H.; Kawai, T.; Sugimoto, M.; Yamashita, M. *Chem. Lett.* **2004**, *33*, 578.
- (7) (a) Robertson, N.; McGowan, C. A. *Chem. Soc. Rev.* **2003**, *32*, 96. (b) Tagami, K.; Tsukada, M. *Jpn. J. Appl. Phys.* **2003**, *42*, 3606. (c) Tagami, K.; Tsukada, M. *Thin Solid Films* **2004**, *464–465*, 429.
- (8) (a) Anderson, H. L.; Martin, S. J.; Bradley, D. D. C. *Angew. Chem., Int. Ed. Engl.* **1994**, *33*, 655. (b) Qureshi, F. M.; Martin, S. J.; Long, X.; Bradley, D. D. C.; Henari, F. Z.; Blau, W. J.; Smith, E. C.; Wang, C. H.; Kar, A. K.; Anderson, H. L. *Chem. Phys.* **1998**, *231*, 87. (c) Thorne, J. R. G.; Kuebler, S. M.; Denning, R. G.; Blake, I. M.; Taylor, P. N.; Anderson, H. L. *Chem. Phys.* **1999**, *248*, 181. (d) Kuebler, S. M.; Denning, R. G.; Anderson, H. L. *J. Am. Chem. Soc.* **2000**, *122*, 339. (e) Screen, T. E. O.; Thorne, J. R. G.; Denning, R. G.; Bucknall, D. G.; Anderson, H. L. *J. Am. Chem. Soc.* **2002**, *124*, 9712. (f) Ogawa, K.; Ohashi, A.; Kobuke, Y.; Kamada, K.; Ohta, K. *J. Am. Chem. Soc.* **2003**, *125*, 13356. (g) Drobizhev, M. S.; Stepanenko, Y.; Dzenis, Y.; Karotki, A.; Rebane, A.; Taylor, P. N.; Anderson, H. L. *J. Am. Chem. Soc.* **2004**, *126*, 15352. (h) Karotki, A.; Drobizhev, M.; Dzenis, Y.; Taylor, P. N.; Anderson, H. L.; Rebane, A. *Phys. Chem. Chem. Phys.* **2004**, *6*, 7.
- (9) Beljonne, D.; O'Keefe, G. E.; Hamer, P. J.; Friend, R. H.; Anderson, H. L.; Brédas, J. L. *J. Chem. Phys.* **1997**, *106*, 9439.
- (10) (a) Shediach, R.; Gray, M. H. B.; Uyeda, H. T.; Johnson, R. C.; Hupp, J. T.; Angiolillo, P. J.; Therien, M. J. *J. Am. Chem. Soc.* **2000**, *122*, 7017. (b) Susumu, K.; Duncan, T. V.; Therien, M. J. *J. Am. Chem. Soc.* **2005**, *127*, 5186.
- (11) (a) Zhou, X.; Ren, A.-M.; Feng, J.-K.; Liu, X.-J.; Zhang, Y.-D. *ChemPhysChem* **2003**, *4*, 991. (b) Zhou, X.; Ren, A.-M.; Feng, J.-K. *Chem. Eur. J.* **2004**, *10*, 5623.
- (12) Stranger, R.; McGrady, J. E.; Arnold, D. P.; Lane, I.; Heath, G. A. *Inorg. Chem.* **1996**, *35*, 7791.
- (13) Arnold, D. P.; Heath, G. A.; James, D. A. *J. Porphyrins Phthalocyanines* **1999**, *3*, 5.
- (14) Arnold, D. P.; Heath, G. A. *J. Am. Chem. Soc.* **1993**, *115*, 12197.
- (15) Arnold, D. P.; Heath, G. A.; James, D. A. *New J. Chem.* **1998**, *22*, 1377.
- (16) Arnold, D. P.; Hartnell, R. D.; Heath, G. A.; Newby, L.; Webster, R. D. *Chem. Commun.* **2002**, 754.
- (17) (a) Li, Z.; Beatty, A. M.; Fehlner, T. P. *Inorg. Chem.* **2003**, *42*, 5707. (b) Li, Z.; Fehlner, T. P. *Inorg. Chem.* **2003**, *42*, 5715.
- (18) Launay, J.-P. *Chem. Soc. Rev.* **2001**, *30*, 386.
- (19) (a) Mack, J.; Stillman, M. J. *J. Porphyrins Phthalocyanines* **2001**, *5*, 67. (b) Mack, J.; Stillman, M. J. *J. Am. Chem. Soc.* **1994**, *116*, 1292.
- (20) Kobayashi, N.; Lam, H.; Nevin, W. A.; Janda, P.; Leznoff, C. C.; Koyama, T.; Monden, A.; Shirai, H. *J. Am. Chem. Soc.* **1994**, *116*, 879.
- (21) (a) Frisch, M. J.; Trucks, G. W.; Schlegel, H. B.; Scuseria, G. E.; Robb, M. A.; Cheeseman, J. R.; Montgomery, J. A., Jr.; Vreven, T.; Kudin, N.; Burant, J. C.; Millam, J. M.; Iyengar, S. S.; Tomasi, J.; Barone, V.; Mennucci, B.; Cossi, M.; Scalmani, G.; Rega, N.; Petersson, G. A.; Nakatsuji, H.; Hada, M.; Ehara, M.; Toyota, K.; Fukuda, R.; Hasegawa, J.; Ishida, M.; Nakajima, T.; Honda, Y.; Kitao, O.; Nakai, H.; Klene, M.; Li, X.; Knox, J. E.; Hratchian, H. P.; Cross, J. B.; Adamo, C.; Jaramillo, J.; Gomperts, R.; Stratmann, R. E.; Yazyev, O.; Austin, A. J.; Cammi, R.; Pomelli, C.; Ochterski, J. W.; Ayala, P. Y.; Morokuma, K.; Voth, G. A.; Salvador, P.; Dannenberg, J. J.; Zakrzewski, V. G.; Dapprich, S.; Daniels, A. D.; Strain, M. C.; Farkas, O.; Malick, D. K.; Rabuck, A. D.; Raghavachari, K.; Foresman, J. B.; Ortiz, J. V.; Cui, Q.; Baboul, A. G.; Clifford, S.; Cioslowski, J.; Stefanov, B. B.; Liu, G.; Liashenko, A.; Piskorz, P.; Komaromi, I.; Martin, R. L.; Fox, D. J.; Keith, T.; Al-Laham, M. A.; Peng, C. Y.; Nanayakkara, A.; Challacombe, M.; Gill, P. M. W.; Johnson, B.; Chen, W.; Wong, M. W.; Gonzalez, C.; Pople, J. A. *Gaussian 03*, Revision B.05; Gaussian, Inc.: Pittsburgh, PA, 2003. (b) Some additional work was done with other minor revisions of Gaussian 98 and Gaussian 03. Details can be obtained from the corresponding author.
- (22) Becke, A. D. *J. Chem. Phys.* **1993**, *98*, 5648.
- (23) (a) Lee, C.; Yang, W.; Parr, R. G. *Phys. Rev. B* **1988**, *37*, 785. (b) Miehlich, B.; Savin, A.; Stoll, H.; Preuss, H. *Chem. Phys. Lett.* **1989**, *157*, 200.
- (24) (a) McLean, A. D.; Chandler, G. S. *J. Chem. Phys.* **1980**, *72*, 5639. (b) Krishnan, R.; Binkley, J. S.; Seeger, R.; Pople, J. A. *J. Chem. Phys.* **1980**, *72*, 650.
- (25) (a) Wachters, A. J. H. *J. Chem. Phys.* **1970**, *52*, 1033. (b) Hay, P. J. *J. Chem. Phys.* **1977**, *66*, 4377.
- (26) Raghavachari, K.; Trucks, G. W. *J. Chem. Phys.* **1989**, *91*, 1062.
- (27) Arnold, D. P.; James, D. A.; Kennard, C. H. L.; Smith, G. *J. Chem. Soc., Chem. Commun.* **1994**, 2131.
- (28) Taylor, P. N.; Anderson, H. L. *J. Am. Chem. Soc.* **1999**, *121*, 11538.
- (29) For example: (a) Low, P. J.; Paterson, M. A. J.; Puschmann, H.; Goeta, A. E.; Howard, J. A. K.; Lambert, C.; Cherryman, J. C.; Tackley, D. R.; Leeming, S.; Brown, B. *Chem. Eur. J.* **2004**, *10*, 83. (b) Barlow, S.; Risko, C.; Coropceanu, V.; Tucker, N. M.; Jones, S. C.; Levi, Z.; Khurstalev, V. N.; Antipin, M. Y.; Kinnibrugh, T. L.; Timofeeva, T.; Marder, S. R.; Bredas, J.-L. *Chem. Commun.* **2005**, 764.
- (30) Heath, G. A.; Arnold, D. P. Unpublished results.
- (31) Halasinski, T. M.; Weisman, J. L.; Ruiterkamp, R.; Lee, T. J.; Salama, F.; Head-Gordon, M. *J. Phys. Chem. A* **2003**, *107*, 3660.
- (32) Robin, M. B.; Day, P. *Adv. Inorg. Chem. Radiochem.* **1967**, *10*, 247.
- (33) Nelsen, S. F. *Chem. Eur. J.* **2000**, *6*, 581.
- (34) Brunschwig, B. S.; Creutz, C.; Sutin, N. *Chem. Soc. Rev.* **2002**, *31*, 168.
- (35) Dreuw, A.; Head-Gordon, M. *J. Am. Chem. Soc.* **2004**, *126*, 4007.